Article:
Gibson, U.J., Holiday, L.F., Allwood, D.A. et al. (2 more authors) (2007) Enhanced longitudinal magnetooptic Kerr effect contrast in nanomagnetic structures. IEEE Transactions on Magnetics, 43 (6). pp. 2740-2742. ISSN 0018-9464

https://doi.org/10.1109/TMAG.2007.894003

Enhanced Longitudinal Magnetooptic Kerr Effect Contrast in Nanomagnetic Structures

Ursula. J. Gibson[1], Lindsay F. Holiday[1], Dan A. Allwood[2], Swaraj Basu[2], and Paul W. Fry[3]

[1]Thayer School of Engineering, Dartmouth College Hanover, Hanover, NH 03755-8000 USA
[2]Department of Engineering Materials, University of Sheffield, Sheffield S1 3JD, U.K.
[3]Centre for Nanoscience and Technology, University of Sheffield, Sheffield S3 7HQ, U.K.

We report on enhanced longitudinal magnetooptic Kerr effect signal contrast in thin-film nanomagnetic disks with in-plane magnetization when combined with dielectric layers that provide impedance matching to the structure and the underlying substrate. Kerr signals can increase by a factor of three, while substrate reflectance is almost completely suppressed. This leads to an increase in Kerr ellipticity relative to the background intensity and a subsequent improvement in the measured signal-to-noise ratio. Measurements using a beam focused on opaque 400-nm Ni disks yield contrast improvements of a factor of 8. Arrays of nanodisks demonstrate more complex behavior due to diffraction effects.

Index Terms—**Antireflection films, dielectric coatings, magnetic nanostructures, magnetooptic Kerr effect (MOKE).**

I. Introduction

THIN-FILM nanomagnetic structures are of interest as both data storage and computational elements [1]–[3], making detection of their in-plane magnetization state essential for fundamental studies of element interactions. Magnetic force microscopy is used extensively for detailed studies of domain structure, while the magnetooptic Kerr effect (MOKE) with focused laser beams is frequently employed for structures larger than a few micrometers [1], [4]. Our goal is to extend the utility of longitudinal MOKE to measurements of smaller structures and/or shorter acquisition times by improvement of the contrast (loop-height-to-average-intensity ratio) by the addition of optical coatings.

Reports of the effect of dielectric overcoats on the contrast in longitudinal MOKE date back to 1958 [5], [6]. However, the largest effort in the application of dielectric layers to improve performance occurred in connection with the development of magnetooptic data storage media [7]–[9], using polar MOKE to measure the out-of-plane magnetized materials. Recently, Qureshi *et al.* [10], [11] explored the use of coatings in measurements of the polar Kerr angle from nanomagnetic structures. We report how antireflection (AR) films can improve longitudinal MOKE contrast for thin-film disks with in-plane magnetization. Furthermore, we demonstrate contrast improvements for a 400-nm disk of a factor of up to 8 under optimum measurement conditions.

II. Experiment

The use of appropriate polarization optics (e.g., analyzing polarizer and quarter-wave retardation plate) allows the Kerr rotation of polarized light reflected from a magnetic surface to be converted into intensity changes. The MOKE signal through a complete magnetization reversal cycle then consists of a large DC component, I_{avg}, and a small magnetization-sensitive component $\mathrm{d}I$. The fractional Kerr signal $\mathrm{dI}/I_{\mathrm{avg}}$ is important as it is often proportional to the signal-to-noise ratio of a measurement system [1].

We used two similar MOKE magnetometers [1] for our measurements, each with a continuous-wave laser source and a 45° angle of incidence. Ni films were measured at a wavelength of 635 nm, focused to a 7 μm $\times$ 10 μm (FWHM) spot on the sample substrate. $Ni_{81}Fe_{19}$ films were measured at 532 nm, either with a collimated $\sim$2-mm-diameter beam or with lenses to achieve a 4-μm $\times$ 7-μm spot. The wavelengths were simply those available in the two analytical laboratories. Both systems employ a quarter-wave plate prior to the analyzing polarizer to convert Kerr ellipticity into Kerr rotation. Hysteresis loops were obtained by applying magnetic fields to samples using an external electromagnet at 27 Hz.

For an optically opaque layer on a substrate, the optimum MOKE response is obtained by coating with a high index material [12]. However, as the size of the magnetic structure is reduced, eliminating as much of the substrate contribution as possible from the average intensity becomes the dominant concern in improving the Kerr contrast. In our experiments, we fabricated the nanodisks on Si(001) substrates using electron beam lithography and lift-off, and then coated the substrate and disks with a single layer of ZnS. ZnS is a readily available material and is near-perfect for p-polarized antireflection coatings on Si at 45° for improving MOKE signals from magnetic structures. Films were deposited either by sputtering or thermal evaporation.

III. Results and Discussion

1-mm $\times$ 1-mm arrays of 1-μm-diameter, 10-nm-thick $Ni_{81}Fe_{19}$ (plus 2-nm Au cap) disks with a 4-μm pitch were coated with different thicknesses of ZnS. Fig. 1 shows the response of these films under focused 532-nm light. All of the traces have the characteristic peak in $\mathrm{d}I/I_{\mathrm{avg}}$, the position of which is dependent upon the Kerr rotation, the average reflected intensity, and the degree of depolarization across the reflected beam [1]. Significant depolarization can result from the curved surfaces of optics and the range of angles a focused beam makes when incident on a tilted surface in MOKE measurements with focused beams. The magnitude of $\mathrm{d}I/I_{\mathrm{avg}}$ is increased twofold,

Digital Object Identifier 10.1109/TMAG.2007.894003

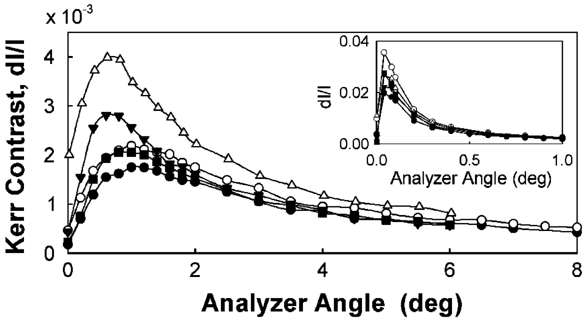

Fig. 1. Kerr contrast from arrays of 1-μm-diameter Ni–Fe dots coated with ZnS films of various thickness as a function of analyzer angle using a 4-μm × 7-μm focused spot for measurement (ZnS thickness: •: 0 nm; ○: 40 nm; ▼: 50 nm; △: 60 nm; ■: 70 nm). The inset shows repeat measurements using a 2-mm collimated beam. Lines are guides to the eye.

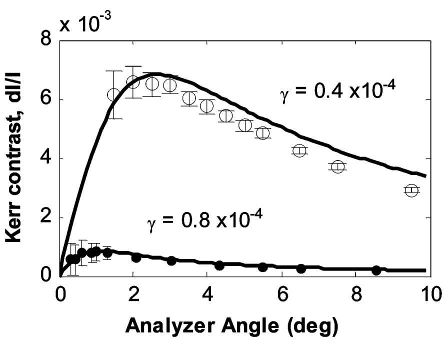

Fig. 2. Kerr signal $\mathrm{d}I/I$ as a function of analyzer angle ϕ obtained from a single 400-nm-diameter Ni disk uncoated (•) and coated (○) with 58-nm ZnS and using a 7-μm × 10-μm focused spot for measurement. Curves are fits using (2) with values for the depolarization factor γ shown above.

and the depolarization is decreased (as indicated by the peak shift to lower analyzer angles) for a 60-nm ZnS coating.

Measurements on the coated arrays with an unfocused beam drastically reduced the depolarization of all reflected beams, allowing very high $\mathrm{d}I/I_{\mathrm{avg}}$ values to be obtained at very small analyzer angles (Fig. 1 inset), at the cost of low signal levels. Furthermore, the signal response to coating thickness changes, with a 40-nm ZnS coating producing the largest $\mathrm{d}I/I_{\mathrm{avg}}$. This surprising result, we believe, is due to an enhancement gained from suppressing nonzero diffracted orders and illustrates the complexities present in obtaining an ideal AR coating for magnetooptical measurements.

We also fabricated isolated 22-nm-thick Ni disks with diameters between 400 nm and 10 μm, both with and without a 58-nm ZnS layer. The fraction of the beam intensity intercepted was calculated by convoluting the disk dimensions with the elliptical Gaussian beam profile. Fig. 2 shows the Kerr contrast dI/I_{avg} as a function of analyzer angle for a coated and uncoated 400-nm-diameter disk.

The AR coating has a significant effect on the measured signal, increasing $\mathrm{d}I/I_{\mathrm{avg}}$ by a factor of 8. The improvements for 5- and 2-μm-diameter disks were factors of 4 and 6, respectively, indicating the importance of the relative size of the disk and laser spot.

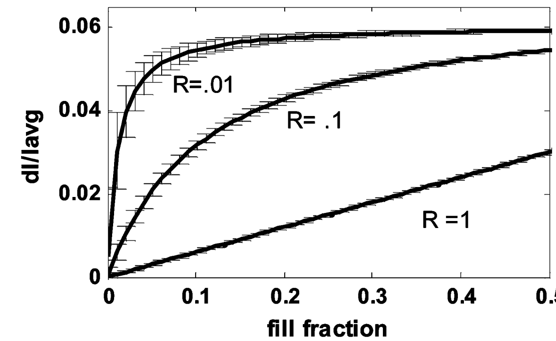

Fig. 3. Modeled $\mathrm{d}I/I_{\mathrm{avg}}$ for different fill fractions. R is in units of the magnetic film's reflectance.

To understand this behavior, we modeled the MOKE contrast on the basis of our experimental configurations [1] and a multilayer calculation of the reflectivity [12] of the films. The simplest averaging approach to calculate the response of a disk on a substrate is an average based on the fraction of the intensity [11], f, that strikes the substrate and the disk.

$$\frac{\mathrm{d}I}{I_{\mathrm{avg}}} = \frac{f\mathrm{d}I_{\mathrm{film}} \pm \text{noise}}{fI_{\mathrm{film}} + (1-f)\,R + q\gamma} \tag{1}$$

where $\mathrm{d}I$ is the height of the Kerr loop, I_{avg} is the mean intensity, I_{film} and $\mathrm{d}I_{\mathrm{film}}$ are the mean intensity and Kerr signal of the equivalent continuous magnetic film, respectively, ϕ is the analyzer angle with respect to the extinction condition, and $\gamma(\sim 10^{-4})$ is the depolarized component. R is the Fresnel reflectance of the (coated) substrate structure. Reductions in R and γ lead to improvements in contrast for small spots; q represents a reduction in the depolarization term that should scale with the reductions in R and I_{film}. Noise contributions are included, as the noise floor presents a hard limit to the ability to measure the Kerr signal. The functional form of (1) is plotted in Fig. 3 for several values of the parameter R with the noise value and analyzer angle ϕ held constant, and the Kerr reflection coefficient being small compared with the total Fresnel reflection coefficient ($r_{\mathrm{ps}} \ll r_{\mathrm{pp}}$). Several things become clear in this simple formulation. As expected, if the reflectance of the substrate is equivalent to that of the magnetic material, there will be a linear reduction in $\mathrm{d}I/I_{\mathrm{avg}}$ as the fill fraction is reduced. If the substrate has a lower reflectance than the magnetic material, the overall intensity drops more rapidly than the linear loss of $\mathrm{d}I_{\mathrm{film}}$, leading to a delayed roll-off in the Kerr contrast. However, even though the contrast can be maintained near the level of a beam-filling film, the uncertainty in the measurement becomes large when the noise and signal levels become comparable.

An alternative approach is to consider the various reflected field amplitudes, including any cross-terms. The equation describing the Kerr contrast, not including diffraction, is

$$\frac{\mathrm{d}I}{I_{\mathrm{avg}}} = \frac{4[f^2E_{\mathrm{pp}} + f(1-f)E_{\mathrm{sub}}]E_{\mathrm{ps}}\sin(\phi)\cos(\phi) \pm \text{noise}}{[fE_{\mathrm{pp}} + (1-f)E_{\mathrm{sub}}]^2\sin^2(\phi) + f^2E_{\mathrm{ps}}\cos^2(\phi) + q\gamma} \tag{2}$$

where E_{pp} and E_{ps} are the Fresnel and Kerr components of the field and E_{sub} is the Fresnel component from the substrate.

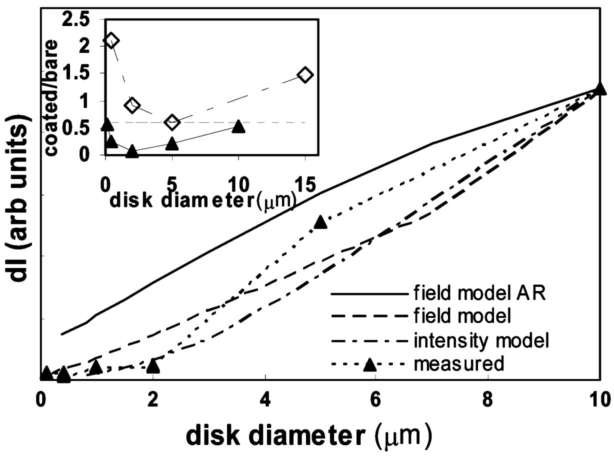

Fig. 4. Magnitude of $\mathrm{d}I$ as a function of disk diameter for Ni on Si, with calculations for an intensity averaging model, and a field amplitude model with an uncoated and coated Si substrate. The inset shows the ratio of slopes of $\mathrm{d}I$ versus $\sin(\phi I)\cos(\phi)$ for coated (58-nm ZnS) and uncoated Ni disks as a function of disk diameter. (◊: measured data; ♦: amplitude model. The dashed line is the prediction of the intensity model.)

(N.B. The expression is evaluated by taking the absolute value of the products, and the substrate contribution is not necessarily in phase with that of the disk.) As the size of the disk decreases relative to the wavelength, diffraction effects become important and the signal $\mathrm{d}I$ falls off more rapidly than predicted by a plane-wave treatment of amplitude terms. Fig. 4 shows the measured reduction in $\mathrm{d}I$ for Ni on Si (uncoated) as a function of disk diameter and compares this with the predicted values from both the intensity and field models, normalized to the 10-μm disk. From this plot, the fit to experimental data appears reasonable for both models, indicating that the simpler intensity based model could be used conveniently. However, the inset shows a plot of the ratio of the slope of $\mathrm{d}I$ versus $\cos(\phi)\sin(\phi)$ for coated and uncoated disks of several sizes that is useful in determining which model is most appropriate (N.B. the "15-μm" data point is for a continuous film). In the intensity formulation, the ratio of the coated and uncoated slopes is independent of disk size, but the measured slope data follow the shape of the field-predicted curve, with a slight vertical offset, and a minimum at a higher disk size than predicted. The vertical displacement may be due to differences in the model parameters and the actual dielectric properties of the films, and the shift to higher diameters is consistent with diffractive losses.

IV. Conclusion

We have shown how antireflection dielectric coatings can be used to improve the MOKE signals obtained from magnetic nanostructures with in-plane magnetization. The level of improvement depends not only upon the dielectric properties of the materials but also on the relative size of the magnetic structure and the laser probe beam diameter. These are best described by a model describing the interaction of the various amplitude reflection coefficients rather than a simple intensity averaging approach. We observed a factor of 8 increase in the contrast for a 400-nm disk and predict larger enhancements for smaller structures, making the use of antireflection coatings of interest to a wide range of researchers within nanoscale magnetism.

Acknowledgment

This work was supported by NIST Grant No. 6NANB2D0120 and the EPSRC under Advanced Research Fellowship No. GR/T02942/01 and Grant No. GR/T02959/01. The authors would like to thank S. Bowden, J. Cui, and T. Davis for help with sample preparation, and M. Testorf and E. Hansen for thoughtful discussions.

References

[1] D. A. Allwood, G. Xiong, M. D. Cooke, and R. P. Cowburn, "Magneto-optical Kerr effect analysis of magnetic nanostructures," *J. Phys. D, Appl. Phys.*, vol. 36, pp. 2175–2182, 2003.

[2] A. Imre, G. Csaba, L. Ji, A. Orlov, G. H. Bernstein, and W. Porod, "Majority logic gate for magnetic quantum-dot cellular automata," *Science*, vol. 311, pp. 205–208, 2006.

[3] S. Visnovsky, V. Parizek, M. Nyvlt, P. Kielar, V. Prosser, and R. Krishnan, "Magnetooptical Kerr spectra of nickel," *J. Magn. Magn. Mater.*, vol. 127, pp. 135–139, 1993.

[4] T. J. Hayward, T. A. Moore, D. H. Y. Tse, J. A. C. Bland, F. J. Castano, and C. A. Ross, "Exquisitely balanced thermal sensitivity of the stochastic switching process in macroscopic ferromagnetic ring elements," *Phys. Rev. B*, vol. 72, pp. 184430-1–184430-6, 2005.

[5] J. Kranz and W. Drechsel, "Über die Beobachtung von Weißschen Bereichen in polykristallinem Material durch die vergrößerte magnetooptische Kerrdrehung," *Z. Physik.*, vol. 150, p. 632, 1958.

[6] P. Lissberger, "Kerr magneto-optic effect in nickel-iron films.2. Theoretical," *J. Opt. Soc. Amer.*, vol. 51, p. 957, 1961.

[7] R. Atkinson, I. W. Salter, and J. Xu, "Quadrilayer magnetooptic enhancement with zero Kerr ellipticity," *J. Magn. Magn. Mater.*, vol. 102, pp. 357–364, 1991.

[8] M. Mansuripur, "Analysis of multilayer thin-film structures containing magnetooptic and anisotropic media at oblique-incidence using 2 × 2 Matrices," *J. Appl. Phys.*, vol. 67, pp. 6466–6475, 1990.

[9] K. Balasubramanian, A. S. Marathay, and H. A. Macleod, "Modeling magneto-optical thin-film media for optical-data storage," *Thin Solid Films*, vol. 164, pp. 391–403, 1988.

[10] N. Qureshi, H. Schmidt, and A. R. Hawkins, "Cavity enhancement of the magneto-optic Kerr effect for optical studies of magnetic nanostructures," *Appl. Phys. Lett.*, vol. 85, pp. 431–433, 2004.

[11] N. Qureshi, S. Q. Wang, M. A. Lowther, A. R. Hawkins, S. Kwon, A. Liddle, J. Bokor, and H. Schmidt, "Cavity-enhanced magnetooptical observation of magnetization reversal in individual single-domain nanomagnets," *Nano Lett.*, vol. 5, pp. 1413–1417, 2005.

[12] P. R. Cantwell, U. J. Gibson, D. A. Allwood, and H. A. M. Macleod, "Optical coatings for improved contrast in longitudinal magneto-optic Kerr effect measurements," *J. Appl. Phys.*, vol. 100, pp. 093910-1–093910-9, 2006.

Manuscript received October 31, 2006 (e-mail: Ursula.J.Gibson@Dartmout.edu).